



Cite this: *Polym. Chem.*, 2015, **6**, 738

## Synthesis of thermal and oxidation dual responsive polymers for reactive oxygen species (ROS)-triggered drug release†

Chunsheng Xiao,<sup>a</sup> Jianxun Ding,<sup>a</sup> Lili Ma,<sup>a,b</sup> Chenguang Yang,<sup>a,b</sup> Xiuli Zhuang<sup>a</sup> and Xuesi Chen<sup>\*a</sup>

We demonstrated herein a kind of thermal and oxidation dual responsive polymer with a novel structure of alternating hydrophilic and hydrophobic segments in the backbone. The polymers were facilely synthesized by thiol–ene polymerization of poly(ethylene glycol) diacrylate (PEGDA) and 1,2-ethanedithiol (EDT) monomers. The resulting PEG–EDT copolymers exhibited a sharp and reversible thermal-induced phase transition in aqueous medium which was identified to be caused by the cooperativity of dehydration of PEG segments and the increased hydrophobic interaction between  $\beta$ -thioether ester segments in the backbone. Additionally, the cloud point temperatures of PEG–EDT copolymers were examined to be dependent on the molecular weight of PEG, polymer concentration, addition of NaCl and isotopic solvent. More importantly, the PEG–EDT copolymers were tested to be oxidation sensitive due to the presence of oxidizable thioether groups in the backbone. The collapsed polymers at elevated temperatures could be easily converted into completely water-soluble polymers by oxidative conversion of hydrophobic thioether groups into hydrophilic sulfoxide and sulfone groups. This oxidation-switchable water solubility inspired us to use this copolymer in design of the oxidation-triggered drug delivery system. Thus, a triblock copolymer mPEG-*b*-575EDT-*b*-mPEG was synthesized by a one-pot method. The resulting triblock copolymer could self-assemble into nanoparticles using thermal and oxidation dual responsive 575-EDT as the core and mPEG as the shell. As a consequence, the hydrophobic model drug (*i.e.*, Nile Red) can be effectively encapsulated into the collapsed nanoparticle core at the body temperature while released by oxidation-triggered disruption of the nanoparticles. This tunable thermo-responsive behavior in combination with oxidation-triggerable thioether groups makes these PEG–EDT copolymers promising for reactive oxygen species (ROS) responsive drug delivery.

Received 21st August 2014,  
Accepted 25th September 2014

DOI: 10.1039/c4py01156b

www.rsc.org/polymers

## Introduction

Over the past few decades, stimuli-responsive polymers have recorded great success in the biomedical field including triggered drug/gene delivery, bio-responsive surfaces, bioseparation and diagnostics.<sup>1–7</sup> Among them, thermo-responsive polymers that show an acute phase transition in response to

modest temperature changes have attracted enormous attention, which is mostly due to the fact that the temperature stimulus is easily accessible and closely related to the body.<sup>6,8</sup> Generally, any flexible polymer containing both hydrophilic and hydrophobic moieties is likely to be thermo-responsive in aqueous solution.<sup>9,10</sup> In these polymers, the hydrogen bonds between hydrophilic moieties and water molecules make the polymer soluble in water while the hydrophobic interactions from hydrophobic moieties lead to aggregation of the polymer chains. This balance between the hydrophilicity and the hydrophobicity thus determined the lower critical solution temperature (LCST) of the thermo-responsive polymers.<sup>10</sup> In other words, the LCST can be tuned by carefully adjusting the balance. Indeed, the tuning of LCST has been achieved by incorporating hydrophilic or hydrophobic moieties in the backbones, side chains or end groups.<sup>6,8,11–13</sup> Besides the fine tunable LCST, the combination of the

<sup>a</sup>Key Laboratory of Polymer Ecomaterials, Changchun Institute of Applied Chemistry, Chinese Academy of Sciences, Changchun 130022, P. R. China.

E-mail: xschen@ciac.ac.cn

<sup>b</sup>University of Chinese Academy of Sciences, 19A Yuquan Road, Beijing 100049, P. R. China

†Electronic supplementary information (ESI) available: The synthesis and characterization of PEGDA1k, additional turbidity measurements, FT-IR spectra, GPC curves, TEM images and fluorescence emission spectra. See DOI: 10.1039/c4py01156b

responsiveness to other stimuli and thermo-responsiveness to build up multi-responsive polymers is also highly desirable for biomedical applications, in particular for smart drug delivery.<sup>14–17</sup> The preparation of multi-responsive polymers also can be realized by incorporating other stimuli-responsive components in the backbones, side chains or end groups.<sup>8,16</sup>

As one of the most studied LCST-type thermo-responsive materials, polymers with short oligo(ethylene glycol) (OEG) side chains, such as polymers constructed from OEG methacrylate (OEGMA) or OEG acrylate (OEGA) monomers, have received increasing attention in a broad range of biomedical applications due to their good biocompatibility and superior thermo-responsive behaviors.<sup>11–13,18,19</sup> The comparable biocompatibility of these OEG-contained polymers to linear PEG analogues is attributed to their dense OEG side chains.<sup>11</sup> Versatile and tunable thermo-responsive behaviors can be easily achieved by careful adjustment of the hydrophilic–hydrophobic balance by virtue of powerful controlled radical polymerization (CRP) technologies with selective OEG bearing monomers and other comonomers.<sup>11–13</sup> One potential limitation of these conventional OEG bearing polymers is their non-degradable carbon–carbon backbones, which would hamper their wide adoption for *in vivo* applications. To address this issue, recent advances have also demonstrated a series of OEG-contained thermo-responsive polymers with biodegradable polypeptides or polyester backbones.<sup>20–28</sup> However, even though tremendous efforts have been devoted to these OEG-based polymers, most of them employ the balance between hydrophilic OEG side chains and the hydrophobic backbone; few examples have been focused on linear polymers with the balance between hydrophilic and hydrophobic segments in the backbone.<sup>29–31</sup>

In this work, a kind of linear PEG-based poly( $\beta$ -thioether ester) with a novel structure of alternating hydrophilic PEG segments and hydrophobic  $\beta$ -thioether ester segments in the backbone (PEG-EDT) was designed and facilely synthesized by thiol–ene polymerization. Owing to the balance between hydrophilic and hydrophobic segments in the backbone, the resulting PEG-EDT copolymers were examined to be thermo-responsive and thus named main chain thermo-responsive (MCT) polymers. More interestingly, the oxidizable thioether groups in the hydrophobic  $\beta$ -thioether ester segments can be used as oxidation-triggerable groups to cause switching of the hydrophobic segments into hydrophilic ones by oxidative conversion of hydrophobic thioether groups into hydrophilic sulfoxides or sulfones. The resulting sulfoxides and sulfones containing hydrophilic segments disrupt the hydrophilic–hydrophobic balance in PEG-EDT copolymers and subsequently induce redissolution of the collapsed polymers. This temperature and oxidation dual responsive behaviors further led us to design and construct an oxidation responsive drug delivery system based on the PEG-EDT copolymer. The investigations on the oxidation induced disassociation of the self-assembled nanoparticles and the triggered release behavior were carefully carried out.

## Experimental

### Materials

Poly(ethylene glycol) diacrylate (PEGDA575 with average  $M_n = 575 \text{ g mol}^{-1}$  and PEGDA700 with average  $M_n = 700 \text{ g mol}^{-1}$ ) and poly(ethylene glycol) methyl ether (mPEG2k,  $M_n = 2000 \text{ g mol}^{-1}$ ) were purchased from Sigma-Aldrich Co. LLC. Poly(ethylene glycol) diacrylate with average  $M_n = 1000 \text{ g mol}^{-1}$  (PEGDA1k) was prepared from PEG800 ( $M_n = 800 \text{ g mol}^{-1}$ , Aladdin Industrial Inc., China) and acryloyl chloride (96%, Aladdin Industrial Inc., China), which is detailed in ESI.† mPEG2k-acrylate was prepared as described in the literature.<sup>32</sup> 1,2-Ethanedithiol (EDT, 98+%) was purchased from Alfa Aesar (China) Chemical Co. Ltd. 1,8-Diazabicyclo[5.4.0]-7-undecene (DBU, 98%) was purchased from Adamas Reagent Ltd. Nile Red (>98%) was purchased from Tokyo Chemistry Industry Co. Ltd (Shanghai). Hydrogen peroxide ( $\text{H}_2\text{O}_2$ , 30 wt% in water) and other chemicals were purchased from Sinopharm Chemical Reagent Co. Ltd, China. All chemicals were used as obtained.

### General procedure for thiol–ene polymerization

Typically, PEGDA700 (4.90 g, 7.00 mmol) and EDT (0.692 g, 7.35 mmol) were first dissolved in 50 mL of chloroform. The solution was bubbled with Ar gas for about 15 minutes under gentle stirring. Then, 105  $\mu\text{L}$  of DBU (0.70 mmol) was added and the resulting mixture was bubbled with Ar gas for further 5 minutes. The polymerization was sealed under an Ar atmosphere and conducted at room temperature for 12 h. The polymer was obtained as a waxy solid by precipitation in an excess amount of ethyl ether three times and dried under vacuum for 48 h (4.63 g, 83.3% yield). This polymer generated from thiol–ene copolymerization of PEGDA700 and EDT was denoted as 700-EDT in the following content. Similarly, polymer 575-EDT (a viscous solid, 78.2% yield, prepared from copolymerization of PEGDA575 and EDT) and 1k-EDT (a white solid, 86.4% yield, prepared from copolymerization of PEGDA1k and EDT) were synthesized using the same procedure described above.

### One-pot synthesis of the ABA-type triblock copolymer

PEGDA575 (2.88 g, 5.00 mmol) and EDT (0.518 g, 5.50 mmol) were first dissolved in 50 mL of chloroform. The solution was bubbled with Ar gas for about 10 minutes. Then, DBU (75  $\mu\text{L}$ , 0.5 mmol) was added to initiate the polymerization. The DBU-catalyzed thiol–ene polymerization was allowed to proceed under constant Ar flow for 1 h at room temperature. After that, 1.55 g of mPEG2k-acrylate (0.75 mmol) was added and the mixture was further bubbled for 20 minutes before sealing and stirred overnight at room temperature. The polymer solution was precipitated in an excess amount of ethyl ether and the white precipitate was collected by filtration. After drying under vacuum for 2 h, the crude product was redissolved in 40 mL of deionized water and dialyzed against deionized water for 3 days (molecular weight cut-off (MWCO) = 3500 Da). Finally, the triblock copolymer mPEG-*b*-575EDT-*b*-mPEG was obtained as a white solid after lyophilization (3.08 g).

## Instruments and methods

$^1\text{H}$  NMR spectra of monomers and synthesized polymers were recorded on a Bruker AV 300 MHz NMR spectrometer in  $\text{CDCl}_3$ . The temperature-varied  $^1\text{H}$  NMR spectra were recorded on a Bruker AV 400 MHz NMR spectrometer in  $\text{D}_2\text{O}$ . The melting temperature ( $T_m$ ) of the polymers was obtained using a differential scanning calorimeter (DSC, Q100, TA instruments) at a heating and cooling rate of  $10\text{ }^\circ\text{C min}^{-1}$ . The number and weight-averaged molecular weight ( $M_n$  and  $M_w$ ) and  $\text{PDI} = M_w/M_n$  of polymers were determined by gel permeation chromatography (GPC, using the Waters 515 HPLC pump, Styragel® HT3 plus HT4 columns (500-6M) and the 2414 Refractive Index detector) in  $\text{CHCl}_3$  at an elution rate of  $1.0\text{ mL min}^{-1}$  and an operation temperature of  $35\text{ }^\circ\text{C}$ . A series of polystyrene samples with molecular weights ranging from 1270 to 609 000 Da were used to calibrate the GPC. Matrix assisted laser desorption/ionization-time of flight-mass spectroscopy (MALDI-TOF MS) analysis was carried out on a Autoflex speed TOF/TOF mass spectrometer (Bruker Daltonics, Germany) with a 355 nm Nd:YAG laser and an acceleration voltage of 20 kV using *trans*-2-[3-(4-*tert*-butylphenyl)-2-methyl-2-propenylidene]malononitrile (DCTB) as a matrix. The turbidimetric assay was performed on a UV-Vis spectrometer (Shimadzu UV-2401PC) with a temperature controller (Shimadzu S-1700) at 550 nm. A quartz cuvette with a pathlength of 10 mm, a chamber volume of 700  $\mu\text{L}$  and a PTFE lip were used for the UV-Vis measurements. The cloud-point temperature ( $T_{cp}$ ) was defined as the temperature at which 50% transmittance was observed. Transmission electron microscopy (TEM) images were recorded on a JEOL JEM-1011 transmission electron microscope.

## Oxidation of the PEG-EDT copolymer

The oxidation behavior of the PEG-EDT copolymer at different concentrations of  $\text{H}_2\text{O}_2$  was first assayed by monitoring the turbidity changes of PEG-EDT aqueous solution at  $37\text{ }^\circ\text{C}$ . Briefly, 700  $\mu\text{L}$  of the 700-EDT polymer solution ( $3.0\text{ mg mL}^{-1}$  in deionized water) was added into the cuvette and kept at  $37\text{ }^\circ\text{C}$  for 20 min. After that, 100  $\mu\text{L}$  of  $\text{H}_2\text{O}_2$  at the predetermined concentration was added and the mixture was mixed vigorously using a micropipette for about 5 seconds. The transmittance of the solution was then recorded (550 nm,  $37\text{ }^\circ\text{C}$ ) at every 2 minutes.

The oxidation of the PEG-EDT copolymer was also characterized by  $^1\text{H}$  NMR, FT-IR and GPC measurements. For the  $^1\text{H}$  NMR study, 550  $\mu\text{L}$  of 1k-EDT ( $10.0\text{ mg mL}^{-1}$  in  $\text{D}_2\text{O}$ ) was first placed in the NMR tube, to which 50  $\mu\text{L}$  of  $\text{H}_2\text{O}_2$  with the predetermined concentration in  $\text{D}_2\text{O}$  was added, the spectra of the mixture were then recorded at different time intervals on a Bruker AV 300 MHz NMR spectrometer ( $23\text{ }^\circ\text{C}$ ). For the FT-IR study, 218  $\mu\text{L}$  of hydrogen peroxide (30 wt%) was added to a solution of 1k-EDT (300 mg) in 30 mL of deionized water, and the mixture with the final  $\text{H}_2\text{O}_2$ -sulfur molar ratio of 4 : 1 was stirred at  $37\text{ }^\circ\text{C}$ . At the set time points, 5.0 mL of the solution was withdrawn from the mixture and transferred into a dialysis

bag (MWCO 1000 Da), dialyzing against deionized water for 2 days. All the samples were lyophilized to afford colorless solids, which were then subjected to FT-IR measurements (Bio-Rad Win-IR instrument, KBr pellet method). For GPC analysis, 550  $\mu\text{L}$  of 1k-EDT solution ( $10\text{ mg mL}^{-1}$ ) and 50  $\mu\text{L}$  of  $\text{H}_2\text{O}_2$  solution ( $0.8\text{ mmol mL}^{-1}$ ) were first mixed in each 10 mL plastic centrifuge tube (with the  $\text{H}_2\text{O}_2$ -sulfur molar ratio of 4 : 1). The tubes were kept at  $37\text{ }^\circ\text{C}$  with continuous shaking at 70 rpm. At the preset time interval, one tube was taken out and the polymer solution inside was diluted to  $2.0\text{ mg mL}^{-1}$  with 0.2 M  $\text{NaNO}_3$  aqueous solution, which was then directly used for GPC analysis. The aqueous GPC was performed with a Waters 1515 isocratic HPLC pump, an Ultrahydrogel™ Linear Column (500–10 M) and a 2414 Refractive Index Detector. 0.2 M  $\text{NaNO}_3$  aqueous solution was used as an eluent with a flow rate of  $0.5\text{ mL min}^{-1}$  at  $35\text{ }^\circ\text{C}$ . Linear poly(ethylene glycol)s with molecular weights of 1000–218 000 Da were utilized for calibration of the GPC.

## Thermo- and oxidation-responsive properties of the self-assembled mPEG-*b*-575EDT-*b*-mPEG nanoparticles

The thermo- and oxidation-responsive properties of the self-assembled mPEG-*b*-575EDT-*b*-mPEG nanoparticles were investigated by dynamic light scattering (DLS, using WyattQELS™ plus Wyatt DAWN EOS, Wyatt Technology). A polymer solution with the concentration of  $0.5\text{ mg mL}^{-1}$ , prepared by directly dissolving the polymer in deionized water and equilibrating overnight at  $4\text{ }^\circ\text{C}$ , was used for the DLS measurements.

## Nile Red loading and release

50 mg of the mPEG-*b*-575EDT-*b*-mPEG triblock copolymer dissolved in 2.0 mL of tetrahydrofuran (THF) was mixed with 200  $\mu\text{L}$  of Nile Red solution ( $2.5\text{ mg mL}^{-1}$  in THF). The mixture was added dropwisely to 5.0 mL of saline solution ( $9.0\text{ g L}^{-1}$  NaCl in deionized water) under vigorous stirring at  $37\text{ }^\circ\text{C}$ . The mixture was then transferred to a dialysis bag (MWCO 3500) and dialyzed against a saline solution for 24 h at  $37\text{ }^\circ\text{C}$  to remove the THF solvent. After that, the Nile Red-loaded nanoparticle solution was collected and diluted with a saline solution to a polymer concentration of  $2.0\text{ mg mL}^{-1}$ .

$\text{H}_2\text{O}_2$ -triggered Nile Red release was performed by mixing 2.0 mL of Nile Red-loaded nanoparticle solution with 20  $\mu\text{L}$  of  $\text{H}_2\text{O}_2$  solution and incubating at  $37\text{ }^\circ\text{C}$ . The fluorescence spectra were recorded at different time intervals on a PTI fluorescence spectroscope (Photon Technology International, U.S.A.), equipped with a temperature-controlled cuvette holder (TC 125, Quantum Northwest, U.S.A.).  $\lambda_{\text{ex}} = 550\text{ nm}$  was applied for all measurements.

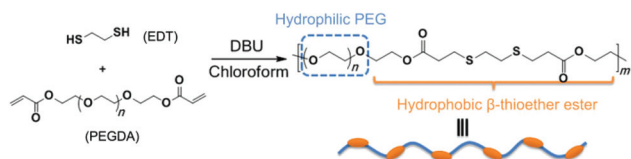
## MTT assay

The MTT (methyl thiazolyl tetrazolium) assay was performed on a mouse fibroblast cell line L929. The cells were seeded with the density of 7000 per well in 200  $\mu\text{L}$  of complete DMEM. After incubation for 48 h, 20  $\mu\text{L}$  of polymer solutions of different concentrations were added. The cells without addition of polymer solutions were used as a control. The cells

were incubated for further 48 h and subsequently subjected to MTT treatment for 4 h. The cell viabilities were then calculated based on the absorbance ratio of samples with and without polymer pretreatments at 480 nm (Bio-Rad 680 microplate reader).

## Results and discussion

The PEG-EDT copolymers were readily synthesized by DBU-catalyzed thiol-ene polymerization of PEGDA and EDT monomers (Scheme 1), which is similar to the previous report.<sup>31</sup> The structure of the obtained polymers was confirmed by <sup>1</sup>H NMR (Fig. 1). The disappearance of resonance peaks from thiol groups (b) and acrylate groups (c, c' and d) and the appearance of resonance peaks at 2.66 (h) and 2.83 (i) ppm demonstrated the successful thiol-ene polymerization and the formation of the  $\beta$ -thioether ester-linked PEG structure in the backbone. The resulting PEG-EDT copolymers were also characterized by GPC and DSC (Table 1). The remarkable increased molecular



Scheme 1 Synthesis of PEG-EDT by thiol-ene polymerization.

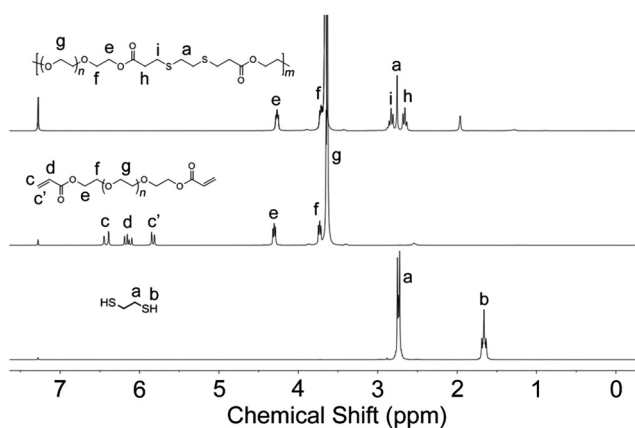


Fig. 1 Typical <sup>1</sup>H NMR spectra of EDT, PEGDA700 and 700-EDT in CDCl<sub>3</sub>.

Table 1 Synthesis and characterization of PEG-EDT copolymers

Polymers	FMR of PEGDA and EDT <sup>a</sup>	$M_n^b$ (g mol <sup>-1</sup> )	PDI <sup>b</sup>	$T_m^c$ (°C)	$T_m$ of PEGDA <sup>c</sup> (°C)
575-EDT	1 : 1	11 900	1.75	— <sup>d</sup>	−11.6
700-EDT	1 : 1.05	80 200	1.79	11.1	14.4
1k-EDT	1 : 1.05	61 500	2.05	25.7	30.4

<sup>a</sup> FMR denotes the feed molar ratio. <sup>b</sup> Measured by GPC in CHCl<sub>3</sub> (1.0 mL min<sup>-1</sup>). <sup>c</sup> Obtained from DSC analysis (second heating). <sup>d</sup> Not detectable.

weight of PEG-EDT copolymers as compared with that of the corresponding PEGDA monomers also verified the formation of PEG-EDT copolymers by thiol-ene polymerization. Additionally, the melting temperatures ( $T_m$ ) of the resulting polymers were slightly lower than that of the corresponding PEGDA monomers (Table 1), which should be ascribed to the disruptive effect of  $\beta$ -thioether ester segments on the crystallization of PEG segments.<sup>33</sup> This result further confirmed the alternating structure of  $\beta$ -thioether ester and PEG segments in the backbone.

The solution properties of as-prepared PEG-EDT copolymers in aqueous medium were then investigated using the turbidimetric assay by UV-Vis spectroscopy. It is interesting to note that all three kinds of PEG-EDT copolymers exhibited a sharp decrease of light transmittance upon heating (*i.e.* LCST-type thermal responsiveness, see Fig. 2A and S2†), while no detectable phase transitions were observed for their corresponding PEGDA monomers even at a temperature as high as 75 °C (Fig. 2B and S3†), which is consistent with the previous report.<sup>31</sup> The distinct differences should be ascribed to the novel structure of alternating hydrophobic  $\beta$ -thioether ester segments and hydrophilic PEG segments in the PEG-EDT backbone. At low temperatures, the hydration of PEG segments made the polymer fully dissolved in water. When the temperature rises, the PEG segments became dehydrated along with the increasing hydrophobic interaction between  $\beta$ -thioether

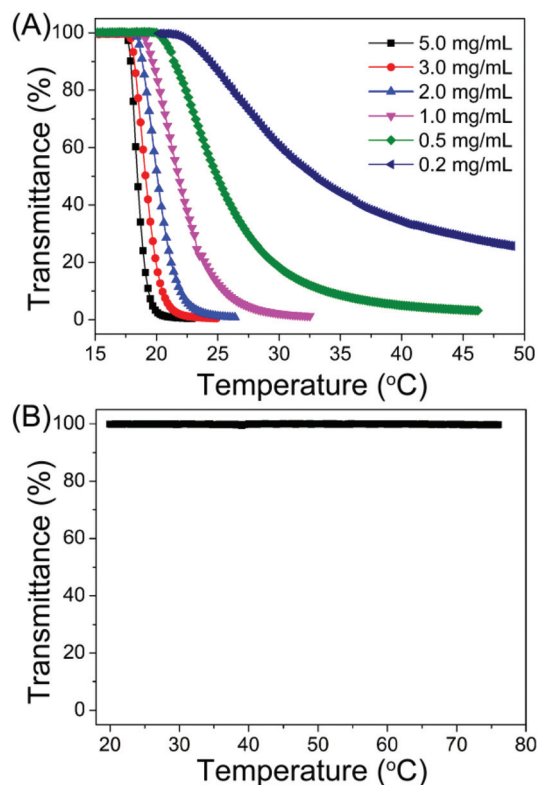


Fig. 2 (A) Temperature-dependent transmittance of 700-EDT solution in deionized water at different concentrations. (B) Temperature-dependent transmittance of PEGDA700 in deionized water (5.0 mg mL<sup>-1</sup>).



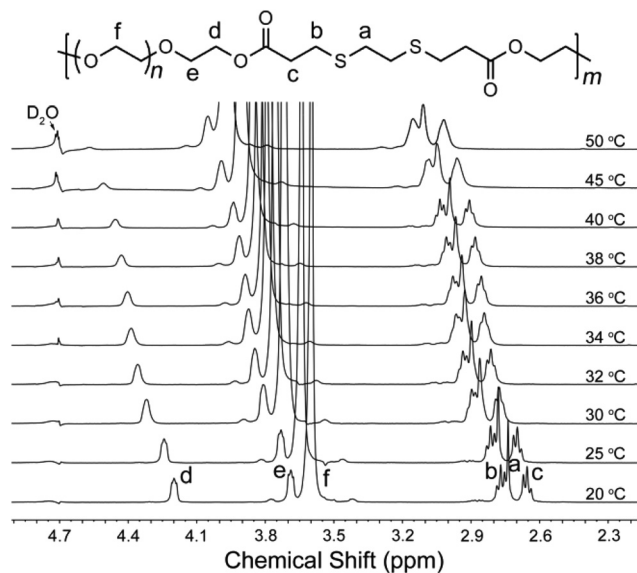


Fig. 3 Variable-temperature  $^1\text{H}$  NMR spectra for 1k-EDT in  $\text{D}_2\text{O}$  ( $5.0 \text{ mg mL}^{-1}$ ).

ester segments, which resulted in the inter- and intra-molecular association and subsequent collapse of polymer chains. To gain more insight into the thermal transition of PEG-EDT aqueous solution, temperature-varied  $^1\text{H}$  NMR measurements were performed and the results are shown in Fig. 3. It is observed that all the resonance peaks from both hydrophobic  $\beta$ -thioether ester and hydrophilic PEG segments were quite resolved at  $20^\circ\text{C}$ , indicating the full dissolution of 1k-EDT in  $\text{D}_2\text{O}$  at low temperatures. Upon raising the temperature, all the resonance peaks shifted to a low field and simultaneously became broader, which should be due to the thermo-induced dehydration of PEG segments and changes of surrounding water molecules near  $\beta$ -thioether ester segments. The decrease of proton d signal intensities was obviously seen at a temperature above  $30^\circ\text{C}$ , which is close to the onset point ( $33^\circ\text{C}$ ) of the thermal transition measured by UV-Vis spectroscopy (Fig. S4 $\dagger$ ), demonstrating the aggregation of polymer chains.<sup>26,34</sup> In other words, the transition of the polymer solution from clear to turbid was caused by the intra- and intermolecular aggregation at elevated temperatures. Furthermore, the tendency of peak shifting to the low field was still observed at a temperature above  $40^\circ\text{C}$ , in which case the thermal transition had finished as measured by the turbidimetric assay (Fig. S4 $\dagger$ ). This result suggests that the dehydration and collapse of polymer chains continually occurred even at the “collapsed state” determined by the traditional turbidity measurements, which is similar to the cases in the previous reports.<sup>26,34–36</sup>

As a LCST-type thermo-responsive polymer, the PEG-EDT copolymers share some common properties with the oligo(ethylene glycol)-contained (co)polymers.<sup>11–13</sup> The thermo-induced transitions were completely reversible and no changes of samples were observed after 9 cycles of heating and cooling processes (Fig. S5 $\dagger$ ). Meanwhile, the cloud point temperatures

( $T_{\text{cp}}$ ) were tested to be depended on the polymer concentration and the molecular weight of the PEG segment (Fig. S6 $\dagger$ ). It is reasonable that the increase of PEG molecular weight in the main chain would increase the hydrophilicity of the polymer, leading to the increase of  $T_{\text{cp}}$ . This property is very comparable to the oligo(ethylene glycol) (meth)acrylate-based copolymers, whose  $T_{\text{cp}}$  is strongly related to the molecular weight of oligo(ethylene glycol) in the side chain.<sup>11,13</sup> Moreover, the decreased  $T_{\text{cp}}$  accompanied by the reduced transition process, as a result of the increasing polymer concentration, should be due to the enhanced intermolecular association in concentrated solution.<sup>30</sup> The influence of NaCl on the thermal transition of PEG-EDT aqueous solution was also investigated by turbidimetry, and a typical “salting out” effect was observed (Fig. S7 $\dagger$ ). The  $T_{\text{cp}}$  gradually reduced as the NaCl concentration increased from 0 to  $18 \text{ g L}^{-1}$ , which should be ascribed to the partial dehydration of polymer chains upon addition of NaCl.<sup>18</sup> Further investigation on the thermo-responsive behavior of PEG-EDT in  $\text{D}_2\text{O}$  was then performed in comparison with that in  $\text{H}_2\text{O}$ . The results revealed that the  $T_{\text{cp}}$  measured in  $\text{D}_2\text{O}$  is roughly  $3\text{--}5^\circ\text{C}$  lower than in  $\text{H}_2\text{O}$  at a polymer concentration above  $0.5 \text{ mg mL}^{-1}$  (Fig. S8 $\dagger$ ). Similar observations have been reported in some other polymers with no strong hydrogen bonding donor.<sup>37–39</sup> And it can be explained by the fact that the hydrophobic interaction between hydrophobic segments is stronger in  $\text{D}_2\text{O}$  than in  $\text{H}_2\text{O}$ ,<sup>40</sup> which subsequently leads to a decrease of the  $T_{\text{cp}}$ .

It is generally accepted that the thermo-responsiveness of the polymer in water is mainly governed by the balance of hydrophilic segment–water hydrogen bonding and segment–segment hydrophobic interactions.<sup>9,10</sup> By introducing specific moieties into the polymer architectures, the hydrophilic–hydrophobic balance could be disrupted, leading to variation of thermo-responsive behaviors. Herein, the presence of thioether groups in the hydrophobic  $\beta$ -thioether ester segments, which can be oxidized to form hydrophilic sulfoxide and sulfone groups,<sup>41–43</sup> has encouraged us to investigate the oxidation responsive behavior of the PEG-EDT copolymers. For this study, a simple turbidity measurement was first applied by monitoring the turbidity changes of the 700-EDT solution upon addition of  $\text{H}_2\text{O}_2$  at  $37^\circ\text{C}$  (Fig. 4). At the test temperature, the 700-EDT solution exhibited minimal light transmittance owing to the collapse of polymer chains. Upon addition of  $\text{H}_2\text{O}_2$ , a sharp transition from turbid to transparent was observed after a period of incubation (see the inset picture in Fig. 4), indicating the oxidation of thioether groups. The oxidation of thioether groups might cause a switch of the hydrophobic  $\beta$ -thioether ester segments into hydrophilic ones and subsequent redissolution of the collapsed polymer. It is also worth noting that the  $\text{H}_2\text{O}_2$ -treated solution remains opaque at the initial incubation and the duration time decreases with the rising concentration of added  $\text{H}_2\text{O}_2$ . As discussed above, the thermo-induced collapse of PEG-EDT chains arises from the dehydration of hydrophilic PEG segments and aggregation of the hydrophobic  $\beta$ -thioether ester segments, which means that the thioether groups are buried in the hydrophobic

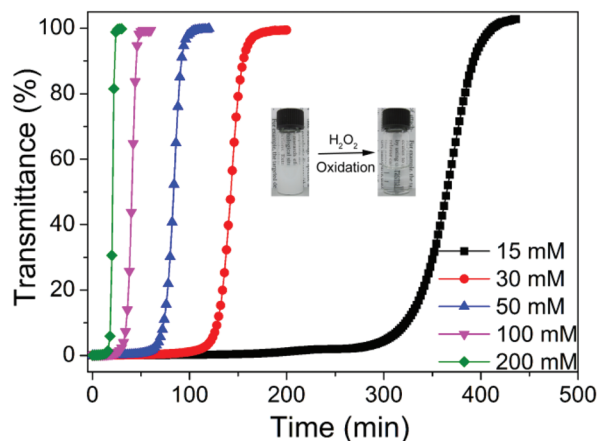


Fig. 4 Turbidity measurements of 700-EDT ( $3.0 \text{ mg mL}^{-1}$ ) in the presence of  $\text{H}_2\text{O}_2$  at  $37^\circ\text{C}$ .

aggregates in the collapsed state. In this case,  $\text{H}_2\text{O}_2$  molecules are less approachable to the thioether groups, as a result the oxidation is slow and the solution keeps turbid. Once the oxidized segments gradually increase to an amount high enough to disrupt the hydrophilic–hydrophobic balance, the collapsed polymer chains redissolve to form a clear solution. To further investigate the solution properties of the oxidized PEG-EDT copolymers, a turbidimetric assay was carried out and the results are shown in Fig. S9.† It is observed that all the oxidized PEG-EDT copolymers were fully soluble in water at temperatures up to  $80^\circ\text{C}$ , indicating that the LCST-type PEG-EDT copolymers were changed into completely water-soluble polymers after oxidation with  $\text{H}_2\text{O}_2$ . This property is different from the previously reported thioether-contained polypeptides, in which case, the oxidation of thioether groups would increase the cloud points.<sup>44</sup>

To deeply understand the oxidation behavior of PEG-EDT copolymers, *in situ*  $^1\text{H}$  NMR measurements were performed. 1k-EDT was selected as the sample for this study since it is fully soluble in water under the testing conditions ( $5.0 \text{ mg mL}^{-1}$ , at  $23^\circ\text{C}$ ). Fig. 5A shows the time dependent  $^1\text{H}$  NMR spectra of 1k-EDT in the presence of four equivalents of  $\text{H}_2\text{O}_2$  per sulfur atom. It is clearly observed that there were two multiple peaks at 2.95–3.15 and 3.15–3.35 ppm, presumably ascribed to methylene groups in the  $\beta$  position of sulfoxides ( $e' + f'$ ) and sulfones ( $e'' + f''$ ), respectively,<sup>45</sup> rising gradually upon addition of  $\text{H}_2\text{O}_2$ . Meanwhile, the gradual disappearance of methylene e and f ( $-\text{CH}_2\text{SCH}_2\text{CH}_2\text{SCH}_2-$ ) at 2.68–2.80 ppm and the shift of methylene d ( $-\text{OC}(\text{O})\text{CH}_2-$ ) from 2.58–2.68 to 2.78–2.89 ppm further verified the oxidation of sulfur atoms by  $\text{H}_2\text{O}_2$ . A slight shift of methylene c to low field was also observed, indicating the solubility changes of the polymer in water, while on ester bond scissions were observed based on the comparison of integrals of methylene c versus methylene a and b (Fig. S10†). The extents of oxidation were then quantitatively estimated by plotting the integrals of methylene  $e' + f' + e'' + f''$  against methylene c and, the results are shown in Fig. 5B. Theoretically, the integral ratio of methylene  $e' + f' + e'' + f''$

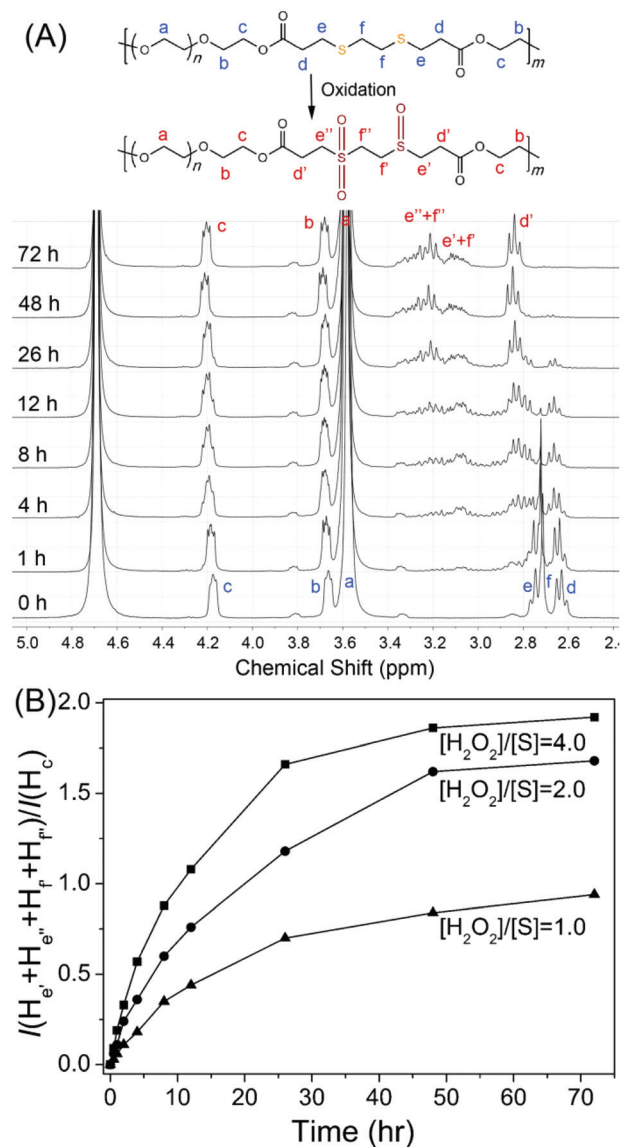
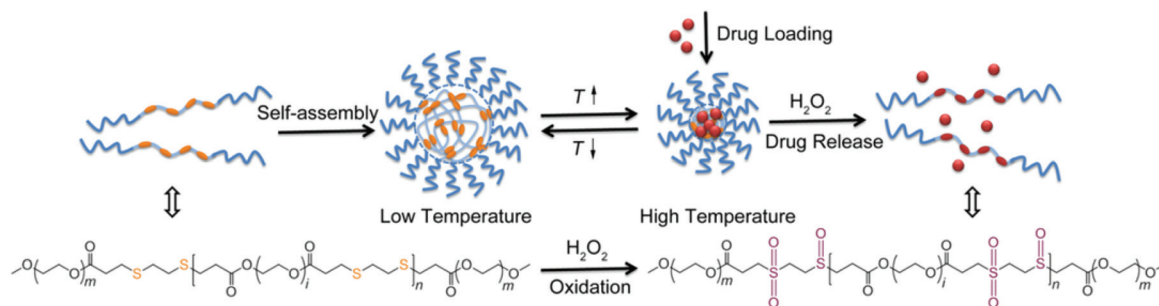


Fig. 5 (A) *In situ*  $^1\text{H}$  NMR spectra of 1k-EDT oxidized by  $\text{H}_2\text{O}_2$  in  $\text{D}_2\text{O}$ , with the  $\text{H}_2\text{O}_2$ /sulfur molar ratio of 4:1 ( $[\text{H}_2\text{O}_2]/[\text{S}] = 4.0$ ). (B) The normalized extents of oxidation as functions of time at different  $\text{H}_2\text{O}_2$ /sulfur molar ratios.

to methylene c should be equal to 2.0, if the sulfur atoms were completely converted to sulfoxides or sulfones. Based on this, the extents of oxidation were calculated to be 96, 84 and 47% for 1k-EDT after 72 h incubation with  $\text{H}_2\text{O}_2$  at  $\text{H}_2\text{O}_2$ /sulfur molar ratios of 4.0, 2.0 and 1.0, respectively. This  $\text{H}_2\text{O}_2$  concentration dependence of oxidation behaviors is similar to the observations in turbidity measurements, *i.e.* the quicker and more extent of oxidation were observed in the sample with higher concentration of  $\text{H}_2\text{O}_2$ . However, the polymers were quickly oxidized upon addition of  $\text{H}_2\text{O}_2$  and no duration time was observed in this case. It might be because that the 1k-EDT was fully dissolved in this condition, so that,  $\text{H}_2\text{O}_2$  could be easily accessible to thioether groups and cause oxidation of them.







**Scheme 3** Self-assembly of the mPEG-*b*-575EDT-*b*-mPEG triblock copolymer and its thermo-responsive and oxidation triggered drug release behaviors.

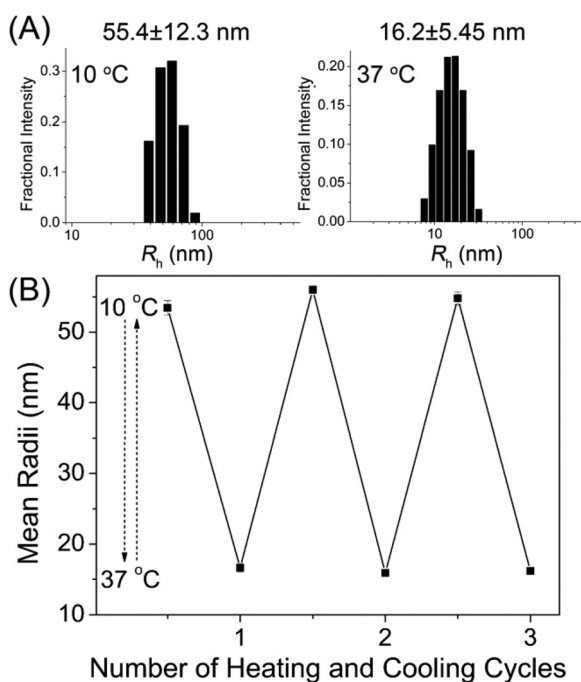


**Fig. 6** (A) DLS results of the mPEG-*b*-575EDT-*b*-mPEG triblock copolymer in aqueous solution ( $0.5 \text{ mg mL}^{-1}$ ) at 10 and 37 °C. (B) Changes of hydrodynamic radii ( $R_h$ ) under repeated heating and cooling. Each point was the average of three measurements.

It has been reported that the reactive oxygen species (ROS) including superoxide,  $\text{H}_2\text{O}_2$  and hydroxide radicals are found to be overproduced in many types of cancer cells.<sup>54–56</sup> Therefore, it is interesting to test the potential application of the  $\text{H}_2\text{O}_2$  responsive mPEG-*b*-575EDT-*b*-mPEG nanoparticles as ROS-targeted anticancer drug delivery vehicles. For this purpose, Nile Red, a hydrophobic dye that has been widely used as a model drug for investigation of stimuli-responsive drug delivery,<sup>57–59</sup> was loaded into the triblock copolymer nanoparticles by a typical dialysis method (with a drug loading efficiency of 16.3%). The oxidation triggered drug release was measured by tracing the fluorescence intensity of Nile Red encapsulated nanoparticles after treatment with  $\text{H}_2\text{O}_2$ . The decrease of fluorescence intensity indicates the release of Nile Red due to its insolubility in aqueous solution.<sup>59</sup> As shown in

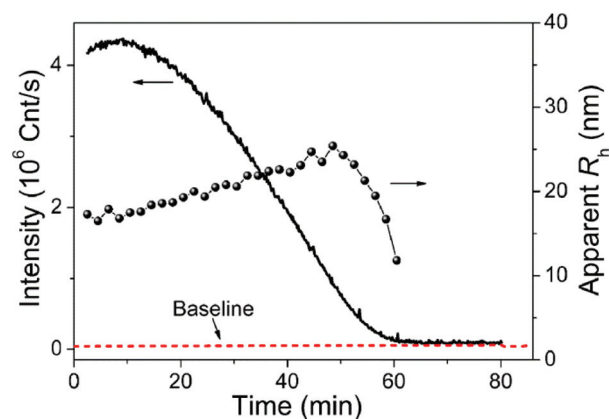


**Fig. 7** Time-dependent light scattering intensity and apparent  $R_h$  of the mPEG-*b*-575EDT-*b*-mPEG triblock copolymer in aqueous solution ( $0.5 \text{ mg mL}^{-1}$ ) upon exposure to 300 mM  $\text{H}_2\text{O}_2$  at 37 °C.

Fig. 8 and S15,<sup>†</sup> in the absence of  $\text{H}_2\text{O}_2$ , no changes of fluorescence intensity were observed throughout the test duration, indicating the good stability of drug-loaded nanoparticles. In contrast, remarkable drug release was observed when treated with  $\text{H}_2\text{O}_2$ , and the higher concentration of  $\text{H}_2\text{O}_2$  would cause quicker release of drug payload. This oxidation triggered release behavior should be ascribed to the  $\text{H}_2\text{O}_2$ -induced disintegration of the nanoparticles that has been previously demonstrated by the DLS study. Moreover, the observation of the loaded Nile Red which precipitated out of solution after  $\text{H}_2\text{O}_2$  treatment (Fig. 8B) and no detectable  $R_h$  in this stage further confirmed that the Nile Red was released as a result of nanoparticle disassociation. These preliminary results suggest that the mPEG-*b*-575EDT-*b*-mPEG nanoparticles are applicable for ROS-responsive anticancer drug delivery.

The cell cytotoxicity of the obtained 1k-EDT before and after oxidation and the mPEG-*b*-575EDT-*b*-mPEG triblock copolymer was estimated by the MTT assay in L929 cells. As shown in Fig. 9, all the polymers exhibited negligible cell cytotoxicity toward L929 cells (>90% cell viability), even at a concentration as high as  $250 \text{ mg L}^{-1}$ . These results suggest good biocompatibility for all the synthesized polymers, which might be attributed to the presence of a large amount of PEG segments in the polymer backbone.



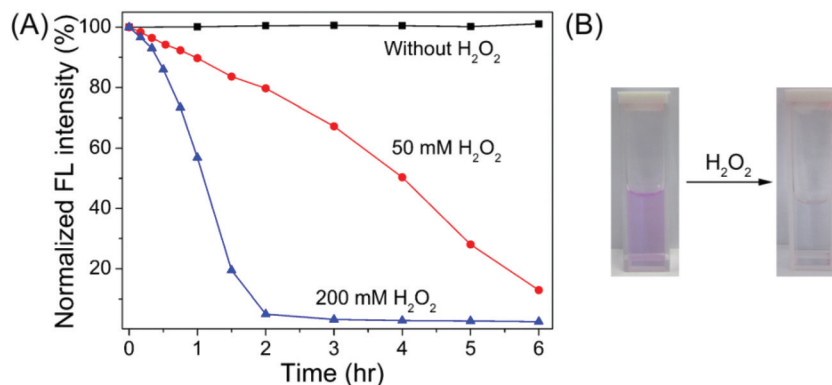


**Fig. 8** (A) Normalized fluorescence intensity of Nile Red encapsulated mPEG-*b*-575EDT-*b*-mPEG nanoparticles (2.0 mg mL<sup>-1</sup> in saline solution) with or without treatment with H<sub>2</sub>O<sub>2</sub>. (B) Digital images of Nile Red encapsulated mPEG-*b*-575EDT-*b*-mPEG nanoparticle solution before and after treatment with 200 mM H<sub>2</sub>O<sub>2</sub>.

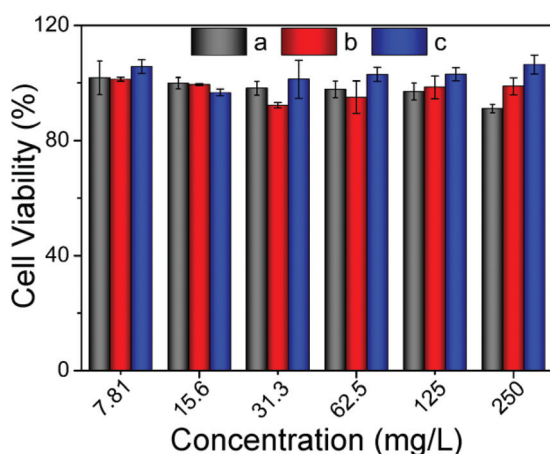


**Fig. 9** Viability of L929 cells cultured with (a) oxidized 1k-EDT (incubated with 4 equivalents of H<sub>2</sub>O<sub>2</sub> per sulfur atom for 26 h), (b) 1k-EDT and (c) mPEG-*b*-575EDT-*b*-mPEG as determined by the MTT assay ( $n = 3$ ).

## Conclusions

In this work, a series of PEG-based poly( $\beta$ -thioether ester)s were readily synthesized by thiol-ene polymerization and tested to be thermo-responsive due to the novel structure of alternating hydrophilic PEG segments and hydrophobic  $\beta$ -thioether ester segments in the backbone. Meanwhile, the resulting PEG-EDT copolymers also exhibited oxidation-responsiveness owing to the presence of oxidizable thioether groups in the hydrophobic segments. Upon oxidation, the thioether groups could be converted into hydrophilic sulfoxides and sulfones, which resulted in the redissolution of PEG-EDT at a temperature higher than its phase transition temperature. Based on these observations, a triblock copolymer mPEG-*b*-575EDT-*b*-mPEG was then synthesized and used for constructing an oxidation responsive drug delivery system. A hydrophobic model drug (*i.e.* Nile Red) could be stably encapsulated into the self-assembled nanoparticles through

the thermo-induced collapse of the 575-EDT segment and released by the way of oxidation triggered disassociation of triblock copolymer nanoparticles. It is also interesting to note that  $\beta$ -thioether ester groups were reported to be sensitive to acid hydrolysis.<sup>32,47</sup> Therefore, this thermal, oxidation and pH multi-responsive PEG-EDT copolymers should be promising for biomedical applications. Additionally, this thermal and oxidation dual responsive polymers based on the novel structure of alternating hydrophilic and hydrophobic segments in the backbone would lead to design of more varieties of multi-responsive materials by simply introducing stimuli-responsive components in the hydrophobic segment.

## Acknowledgements

This work was financially supported by the National Natural Science Foundation of China (51203153, 51303174, 51273196, 51390480, 51233004 and 51321062).

## Notes and references

- S. Ganta, H. Devalapally, A. Shahiwala and M. Amiji, *J. Controlled Release*, 2008, **126**, 187–204.
- P. M. Mendes, *Chem. Soc. Rev.*, 2008, **37**, 2512–2529.
- C. Xiao, H. Tian, X. Zhuang, X. Chen and X. Jing, *Sci. China, Ser. B*, 2009, **52**, 117–130.
- M. A. Stuart, W. T. Huck, J. Genzer, M. Muller, C. Ober, M. Stamm, G. B. Sukhorukov, I. Szleifer, V. V. Tsukruk, M. Urban, F. Winnik, S. Zauscher, I. Luzinov and S. Minko, *Nat. Mater.*, 2010, **9**, 101–113.
- R. de la Rica, D. Aili and M. M. Stevens, *Adv. Drug Delivery Rev.*, 2012, **64**, 967–978.
- E. S. Gil and S. M. Hudson, *Prog. Polym. Sci.*, 2004, **29**, 1173–1222.
- J. Hu and S. Liu, *Macromolecules*, 2010, **43**, 8315–8330.
- D. Roy, W. L. A. Brooks and B. S. Sumerlin, *Chem. Soc. Rev.*, 2013, **42**, 7214–7243.

- 9 V. Aseyev, H. Tenhu and F. M. Winnik, *Adv. Polym. Sci.*, 2011, **242**, 29–89.
- 10 R. X. Liu, M. Fraylich and B. R. Saunders, *Colloid Polym. Sci.*, 2009, **287**, 627–643.
- 11 J. F. Lutz, *J. Polym. Sci., Part A: Polym. Chem.*, 2008, **46**, 3459–3470.
- 12 C. Weber, R. Hoogenboom and U. S. Schubert, *Prog. Polym. Sci.*, 2012, **37**, 686–714.
- 13 G. Vancoillie, D. Frank and R. Hoogenboom, *Prog. Polym. Sci.*, 2014, **39**, 1074–1095.
- 14 R. Cheng, F. Meng, C. Deng, H.-A. Klok and Z. Zhong, *Biomaterials*, 2013, **34**, 3647–3657.
- 15 Z. Ge and S. Liu, *Chem. Soc. Rev.*, 2013, **42**, 7289–7325.
- 16 P. Schattling, F. D. Jochum and P. Theato, *Polym. Chem.*, 2014, **5**, 25–36.
- 17 C. Xiao, Y. Cheng, Y. Zhang, J. Ding, C. He, X. Zhuang and X. Chen, *J. Polym. Sci., Part A: Polym. Chem.*, 2014, **52**, 671–679.
- 18 J. F. Lutz, O. Akdemir and A. Hoth, *J. Am. Chem. Soc.*, 2006, **128**, 13046–13047.
- 19 J.-F. Lutz, *Adv. Mater.*, 2011, **23**, 2237–2243.
- 20 X. Jiang, M. R. Smith III and G. L. Baker, *Macromolecules*, 2008, **41**, 318–324.
- 21 X. Jiang, E. B. Vogel, M. R. Smith III and G. L. Baker, *Macromolecules*, 2008, **41**, 1937–1944.
- 22 C. Chen, Z. Wang and Z. Li, *Biomacromolecules*, 2011, **12**, 2859–2863.
- 23 Y. Cheng, C. He, C. Xiao, J. Ding, X. Zhuang and X. Chen, *Polym. Chem.*, 2011, **2**, 2627–2634.
- 24 W. Wang, J. Ding, C. Xiao, Z. Tang, D. Li, J. Chen, X. Zhuang and X. Chen, *Biomacromolecules*, 2011, **12**, 2466–2474.
- 25 L.-J. Zhang, B.-T. Dong, F.-S. Du and Z.-C. Li, *Macromolecules*, 2012, **45**, 8580–8587.
- 26 X. Fu, Y. Shen, W. Fu and Z. Li, *Macromolecules*, 2013, **46**, 3753–3760.
- 27 J. R. Kramer and T. J. Deming, *J. Am. Chem. Soc.*, 2014, **136**, 5547–5550.
- 28 J. Ding, L. Zhao, D. Li, C. Xiao, X. Zhuang and X. Chen, *Polym. Chem.*, 2013, **4**, 3345–3356.
- 29 X. J. Lu, K. D. Cremeans, H. D. Tang, E. A. Van Kirk, W. J. Murdoch and Y. Q. Shen, *Abstr. Am. Chem. Soc.*, 2009, 237.
- 30 L. Gu, Y. G. Gao, Y. S. Qin, X. S. Chen, X. H. Wang and F. S. Wang, *J. Polym. Sci., Part A: Polym. Chem.*, 2013, **51**, 282–289.
- 31 N. Wang, A. Dong, M. Radosz and Y. Shen, *J. Biomed. Mater. Res., Part A*, 2008, **84A**, 148–157.
- 32 K. Dan and S. Ghosh, *Angew. Chem., Int. Ed.*, 2013, **52**, 7300–7305.
- 33 X. J. Loh, X. Wang, H. Li, X. Li and J. Li, *Mater. Sci. Eng., C*, 2007, **27**, 267–273.
- 34 S. Sun and P. Wu, *Macromolecules*, 2013, **46**, 236–246.
- 35 S. H. Jung, H. Y. Song, Y. Lee, H. M. Jeong and H. I. Lee, *Macromolecules*, 2011, **44**, 1628–1634.
- 36 L. Liu, W. Li, K. Liu, J. Yan, G. Hu and A. Zhang, *Macromolecules*, 2011, **44**, 8614–8621.
- 37 C. Diab, Y. Akiyama, K. Kataoka and F. M. Winnik, *Macromolecules*, 2004, **37**, 2556–2562.
- 38 J. Sun, Y. Peng, Y. Chen, Y. Liu, J. Deng, L. Lu and Y. Cai, *Macromolecules*, 2010, **43**, 4041–4049.
- 39 P. Liu, L. Xiang, Q. Tan, H. Tang and H. Zhang, *Polym. Chem.*, 2013, **4**, 1068–1076.
- 40 F. M. Winnik, *J. Phys. Chem.*, 1989, **93**, 7452–7457.
- 41 S. H. Lee, M. K. Gupta, J. B. Bang, H. Bae and H.-J. Sung, *Adv. Healthcare Mater.*, 2013, **2**, 908–915.
- 42 E. Lallana and N. Tirelli, *Macromol. Chem. Phys.*, 2013, **214**, 143–158.
- 43 A. Napoli, M. Valentini, N. Tirelli, M. Muller and J. A. Hubbell, *Nat. Mater.*, 2004, **3**, 183–189.
- 44 X. Fu, Y. Ma, Y. Shen, W. Fu and Z. Li, *Biomacromolecules*, 2014, **15**, 1055–1061.
- 45 P. Carampin, E. Lallana, J. Laliturai, S. C. Carroccio, C. Puglisi and N. Tirelli, *Macromol. Chem. Phys.*, 2012, **213**, 2052–2061.
- 46 J. Vandenberg, K. Ranieri and T. Junkers, *Macromol. Chem. Phys.*, 2012, **213**, 2611–2617.
- 47 Q. Jin, T. Cai, H. Han, H. Wang, Y. Wang and J. Ji, *Macromol. Rapid Commun.*, 2014, **35**, 1272–1378.
- 48 N. Zaquen, B. Wenn, K. Ranieri, J. Vandenberg and T. Junkers, *J. Polym. Sci., Part A: Polym. Chem.*, 2014, **52**, 178–187.
- 49 S. Kim, Y. Shi, J. Y. Kim, K. Park and J.-X. Cheng, *Expert Opin. Drug Delivery*, 2010, **7**, 49–62.
- 50 C. Deng, Y. Jiang, R. Cheng, F. Meng and Z. Zhong, *Nano Today*, 2012, **7**, 467–480.
- 51 A. Kowalczyk, R. Trzcinska, B. Trzebicka, A. H. E. Müller, A. Dworak and C. B. Tsvetanov, *Prog. Polym. Sci.*, 2014, **39**, 43–86.
- 52 X. Huang, F. Du, J. Cheng, Y. Dong, D. Liang, S. Ji, S.-S. Lin and Z. Li, *Macromolecules*, 2009, **42**, 783–790.
- 53 J.-F. Gohy, S. K. Varshney and R. Jérôme, *Macromolecules*, 2001, **34**, 3361–3366.
- 54 D. Trachootham, J. Alexandre and P. Huang, *Nat. Rev. Drug Discovery*, 2009, **8**, 579–591.
- 55 T. P. Szatrowski and C. F. Nathan, *Cancer Res.*, 1991, **51**, 794–798.
- 56 P. T. Schumacker, *Cancer Cell*, 2006, **10**, 175–176.
- 57 W. Chen, F. Meng, F. Li, S.-J. Ji and Z. Zhong, *Biomacromolecules*, 2009, **10**, 1727–1735.
- 58 N. Fomina, C. McFearin, M. Sermsakdi, O. Edigin and A. Almutairi, *J. Am. Chem. Soc.*, 2010, **132**, 9540–9542.
- 59 J.-H. Ryu, S. Jiwpanich, R. Chacko, S. Bickerton and S. Thayumanavan, *J. Am. Chem. Soc.*, 2010, **132**, 8246–8247.